

## EXPERIMENTAL RESEARCH OF PRE-STRESSED REINFORCED- CONCRETE BODY OF NUCLEAR STATION REACTORS

A. KUBANEISHVILI, A.IURATIN

*The experimental part of the work involves both vessel body model and its components' testing to solve structural and technological problems. On the structural components of the roof (floor) and the wall as well as on confined vessel model the issues were being studied concerning the distribution of stresses from various forces occurring both separately and in combination.*

*- on specimens in a shape of circular disk (roof) from the action of prestressed tendons;  
- on a compound wall of cylindrical shells from the pressure of the cement grout injected into the gap in between as well as from the action of the internal working pressure.*

*On the vessel wall component, the technology of cement grout injection into the gap was being tested, preliminary testing being carried out with cylindrical specimens.*

**Key words:** capacity body, pre-stressed reinforcement, cement slurry, plexiglass, reduction, fragment.

### 1. Selecting materials, proportioning grout and concrete

The choice of model material depends on the purpose of modelling. In view of the fact that it is the prestressed high-pressure body with high cracking-resistance that modelling is to be performed for, it may be considered, with sufficient accuracy, as one operating in an elastic stage, the distribution of stresses in concrete following the linear law.

When investigating the performance of a model within linear elasticity range, for example, in simulating the design diagram of a structure, which is worked out in accordance with structural mechanics code, there is no need to employ materials matching those used in actual practice. In this case, geometrical similarity of the relative deformations of the model and its prototype is unnecessary. Moreover, the usage of identical materials in the modelling of reinforced concrete structures will complicate the task of finding the solution to the problem, for it is impossible to establish a strict line of demarcation between elastic and inelastic performance (since the height of compressed concrete zone and the force in every cross-section of the tendons depend on the extent of the latter's loading) and there is no way to determine the design forces. In such cases it is advisable to use elastic materials, for example, plastic (Plexiglas).

Some difficulties arise due to the difference observed in Poisson's ratio. For instance, Poisson's ratio for Plexiglas is twice that of concrete. However, with the states of tension-compression or torsion prevailing in the structure (that is, only normal and tangential stresses are dominant), less strict requirements may be set as regards the equality of Poisson's ratios for the materials of the model and the actual structure, for this will not lead to significant errors (5-10%) [1].

From the above line of reasoning for model material has been selected plexiglass. Its physical and stress-strain properties have been ascertained in testing briquettes with cross-section of 14x20 mm and working part 80 mm. The test data obtained are as follows: ultimate strength  $R=74,5$  MPa, modulus of elasticity  $E=3560$  MPa, Poisson's ratio  $\mu=0,33$  and friction coefficient  $K=0,37$  (friction of metal on Plexiglas).

The data of our experiments as well as those of [2] show that the plastic deformations at stresses below those constituting 0,15 of the ultimate strength are rather small and the probability that they will be developing in time is negligible. This permits to safely use Plexiglass for the modelling of prestressed structure of high-pressure frame operating in elastic stage.

A common low-strength concrete has been employed [3] for the manufacture of roof and wall components (cylindrical shells). For concrete produced by GAC packed aggregate – and – grout process, cement grout has been used in the gap between walls.

Prior to concrete proportioning, cements and inert materials – sand and crushed stone, have been studied following the standing standards [3,4] and subsequent verification has been performed based on world standards [5,6].

In order to ensure optimal filling of the gap throughout the cross-section and around the edges whereby no air cavities or water accumulation occur, the cement grout should have sufficient fluidity and show little or no bleeding. In addition, good fluidity may be ensured by a relatively high water-content, whereas moderate bleeding sets limits on the permissible amount of water in cement grout.

When proportioning concrete mix to meet those erratic requirements, a number of factors affecting its properties should be taken into consideration, in particular, the type of cement, making mortar plasticizers a part of the mix, adequate cement grout strength etc. The challenge was to obtain such cement grout as would satisfy the requirements placed on its properties and thus ensure proper injection.

The main properties of the injected cement grout have been investigated, in particular, viscosity, bleeding, setting time and strength depending on proportions of the concrete mix, presence of admixtures and water-cement ratio.

Tests have been performed with neat cement grout with no admixtures applied as well as with mortar plasticizer LST (commercial-grade ligno-sulfonates).

Included in table 1 are standard test figures for physical and stress-strain properties of the cement supplied by both Caspi and Rustavi cement works [7].

A device similar to that designed in the USA and England [8-10] has been used to determine cement grout viscosity. It was a conical jar 230 mm in height, its exit tube being 13 mm in diameter. The mortar (1800 cu.cm in volume) prepared with cement that had been produced at Caspi cement works, was poured into the jar, filling the entire conical section, whereupon it was released through the exit tube. Prior to filling, the jar walls were being dampened. Cement grout discharge time count was being kept by a stop-watch, which would shut off when cement grout had stopped spouting forth in jets. The time noted has been taken for viscosity characteristic. A device like that, within the ordinary range of cement grout viscosity, provides conventional figures, their comparison only being possible for tests carried out exclusively by means of this type of a device with dimensions specified above.

Table 1

Cement physical and stress-strain properties

Indicator	Cement produced at	
	Caspi cement works	Rustavi cement works
Normal thickness, %	26,75	24,60
Setting time, hr-min:		
Beginning	3-40	1-50
End	6-50	4-20
Volume weight, g/cu.cm	1,06	1,15
Density, g/cu.cm	3,15	3,07
Activity at 7 days/28 days, MPa:		
Compression	38,8/51,2	24,0/41,8
Bending	4,24/7,81	3,15/5,76
Specific surface, sq.cm/g	3570	2850

Table 2 displays figures for viscosity - water-cement ratio relationship with of without admixtures.

As evident from the data included in the above table, cement grout viscosity may vary over a wide range. An application of mortar plasticizer significantly reduces cement grout viscosity.

Included in the same table are the results obtained in determining the intensity of bleeding for the same cement grouts that had been investigated in cylindrical device (a jar with a lid) similar to that used in Germany [10], its diameter being 100 mm and height 130 mm. The said jar was filled up with cement grout to a depth of 100 mm and then covered with a lid to avoid evaporation of separated water. The jar dimensions accepted are best for more intensive bleeding, which makes it possible for this property of cement grout to be better detected in testing.

One important prerequisite to high-quality injection is that there be time enough for the beginning of injected cement grout setting. With this in mind some specific tests have been performed with cement produced at Caspi cement works. By means of Vicat needle setting periods have been determined for cement grouts with differing water-cement ratio and with or without cement grout plasticizer. The results of those tests performed at 15<sup>0</sup>C are represented in table 3.2.

Table 2

The influence of both water-cement ratio and mortar plasticizer on cement grout viscosity, bleeding, strength and setting time

No of mortar	W/C	Admixture, percentage of cement mass	Setting time, hr-min		Strength, MPa		Conventional viscosity, c	Bleeding, %
			Beginning	End	age, days			
					7	28		
1	0,50	-	7-15	12-45	18,5	38,2	15	2,10
2	0,40	-	2-30	8-05	28,7	51,6	21	1,30
3	0,35	-	1-35	6-10	36,7	63,2	-	1,10
4	0,50	0,25	7-45	12-30	19,7	40,2	10	2,50
5	0,40	0,25	3-10	8-40	28,5	54,5	14	1,53
6	0,35	0,25	1-30	6-45	36,4	63,7	20	1,15

The influence of both water-cement ratio and the composition of the injected cement grouts on their strength has been studied in testing cubes of 5x5x5 cm at varying age (7 and 28 days) with normal maturing, t=19<sup>0</sup>C, W=90%. The results obtained are represented in table 2.

An injection of cement grout into the gap between shells preliminarily filled with crushed stone (gravel) results in the formation of concrete known as grouted aggregate concrete (GAC) [12]. There are two ways of accomplishing packed aggregate - and grout process: by gravity grouting (gravitational method), which means that cement grout spreading in coarse aggregate voids occurs under the action of its mass due to high mobility, and by pressure grouting (injection method), wherein the spreading of cement grout in coarse aggregate voids will be ensured by the pressure produced by cement grout pumps.

The first way (gravitational method) involved mix proportioning to fill the gap between cylindrical shells with a view to comparing gap concrete with grouted aggregate concrete produced by the second way (injection method) intended for the creation of various pressures in metallic cylindrical forms.

Physical and stress-strain properties of two sets of grouted-aggregate concrete specimens have been studied with 100x100x100 mm cubes and 100x100x400 mm prisms prepared with cement produced at Caspi cement works (first set) as well as at Rustavi cement works (second set). The first set of specimens (of high strength) are intended for checking the possibility of

grouted aggregate concrete application to actual structures, whereas the second set of specimens - for tests in a laboratory. Test results are represented in table 3.

Table 3

The influence of water-cement ratio on the strength of grouted-aggregate concrete (GAC)

No of a set	No of composition	Concrete composition per 1 cu.m, kg					Strength, MPa			Modulus of elasticity, MPa
		cement	water	crushed stone	plasticizer	W/C	Cube		Prismi	
							specimens	primary standard		
I	1	634	317	1450	1,58	0,50	38,1	36,2	26,0	31000
	2	679	273	1450	1,70	0,40	46,2	43,9	27,8	35200
	3	704	246	1450	1,74	0,35	47,1	44,8	28,7	36100
II	4	634	317	1450	1,58	0,50	21,1	20,0	15,6	20000
	5	679	272	1450	1,70	0,40	32,2	20,6	20,5	27000
	6	704	246	1450	1,74	0,35	38,1	36,2	21,4	28000

Footnote: In converting (100x100x100 mm) cube strength into primary standard specimen (150x150x150 mm) strength, according to GOST 10180-90 [13], a conversion coefficient of 0,95 has been employed.

Class B7,5 and B15 concretes have been designed and produced for vessel body components. Rustavi plant cement has been used for a binding agent. In table 4 are summarized concrete compositions and their physical and stressed-strained indicators obtained for cubes 100x100x100 and prisms 100x100x400 mm.

Table 4

Physical and stress-strain properties of concrete used for model elements

No of composition	Concrete composition per 1 cu.m, kg					Strength, MPa			Modulus of elasticity, MPa
	cement	water	sand	crushed stone	plasticizer	Cube		Prism	
						specimens	primary standard		
1	200	160	900	1140	0,500	11,8	11,2	8,15	16500
2	250	120	850	1180	0,625	23,7	22,5	16,65	23450

## 2. Manufacture of a model and structural components

The model was manufactured from 14 mm thick Plexiglass sheets. To fabricate the outer and inner shells, the sheets 1539x690 mm and 1451x578 mm in size, respectively, were heated up in advance to temperatures below the softening point, with subsequent wrapping on matrixes with diameters corresponding to the internal diameters of the inner and outer shells (414 and 462 mm respectively). After cooling down they were removed from the matrixes and cemented together with dichloritan glue. With a view to increasing the resistance of the glued seams, 1,2 mm thick aluminium strips were fixed along the whole length of the said seams. Joint operation of those sheets and the cylindrical surface was made possible by 3 mm dia. screws.

The roof and the floor of the frame were assembled from four disks 442 mm in diameter, the overall thickness being 56 mm. The central part of the disks had curvilinear grooves (Fig. 1) with 2 mm depressions wherein 1,7 mm dia. concrete reinforcement wires with tread cut at the ends were laid prior to assemblage.



Fig. 1. Model view from above



Fig. 2. General view of the model

Joint operation of the disks was made possible by dikchloritane glue and screws. The same technique has been employed to attach the floor and roof so prepared to the ends of the inner shells (Screws  $d=4$  mm).

Two holes with a tread were provided in the frame roof, into which, before model testing for internal pressure, the standard pressure gauge was subsequently screwed in for monitoring the pressure applied along with a pipe union with a hose attached for water pressure feed (Fig. 1).

The model inner shell with free length of concrete reinforcement wire is inserted in - to the outer shell, wherein 4 mm dia. holes were drilled in advance to let the tendons run through.

On the outside of the outer shell, at tendon exit points, plexiglass gaskets were secured with glue to ensure a close contact between the tendons and the shell by means of screwed-on nuts.

These nuts will serve as grippers in the process of model compressive stressing and testing for internal pressure.

To study the stressed-strained state of closed-type inner and outer shells in the process of compressive stressing through spreading the expanding alunite cement into the gap between the inner and outer shells, electric strain gauges with 20 mm base were glued to the inner surface of the inner shell as well as to the inside of the roof and the floor before final assemblage so that a rather accurate determination of the stressed state of the entire interior part of the frame could be made possible.

Bearing in mind frame symmetry, the said strain gauges were chiefly grouped in one fourth part of the disk but in order to monitor the readings, they were installed in other parts of the disk as well. The wires extending from the sensors to the automated strain gauge were run through the holes in the roof. Altogether there were on the inner part there were 56 strain gauges attached. Fig.2 represent the general view of the model.

To study the properties of the concrete (GAC) firming under pressure in a hermetic gap between the inner and outer frame shells, six metallic sectional cylindrical forms of diameter 150 mm and 450 mm in height have been manufactured (Fig.3). The form was assembled of two semi-cylinders and two circular flanges. On the semi-cylinder ends circular stiffening ribs were welded.

At assembling of semi-cylinder forms were four bolts and a rubber strap and bolted together glued along the joint from the inside to ensure hermetic sealing. Afterwards both the upper and the lower flanges with cover gaskets are mounted and tied to the form with four lengthwise bolts. Before mounting the upper flange, the mould cavity is filled with crushed stone. Two holes with a thread are allowed in the upper flange - one for setting up a manometer controlling the pressure in the form at cement grout injection, and another one, for air release, that is being plugged at cement grout discharge. Upon termination of injection the valve cuts off the flow, fixing the registered pressure.

To determine the influence of casing rigidity on concrete strength indices (GAS) forms have been manufactured simultaneously from plastic pipes with 100 mm in diameter and 450 mm in height, concrete curing under pressure being done on spring devices. These forms (8 pieces) had 30 mm thick concrete floors. In order to ensure the action of pressure on the freshly-placed concrete, concrete punches have been moulded in advance serving as a piston, in 80 mm long pipes cut off the main form pipe (fig.4).

For punches as well as for form bottoms class B25 concrete has been used with a view to investigating proposed deformations of concrete hardening under pressure in a gap between shells, causing a drop in prestress, 20 mm thick reinforced concrete hollow cylinders, 450 mm in height with a diameter of 100 mm, have been manufactured, the reinforcement being done with a spiral of wire 2 mm in diameter and 20 mm pitch. In contrast to above-mentioned specimens, the curing of concrete produced in reinforced concrete casings proceeded in the same spring devices, with pressure exerted by punches positioned on either end of the cylinder. In order to ensure the maximum of air-tightness in the body of the cylinder under the application of pressure to the concrete, at either end of the cylinder on the inside, plastic tube pieces 25 mm in length were glued with epoxy adhesive, the said pieces being cut from the same pipes as were used for the punches. All in all, there were 8 cylinder specimens fabricated along with their punches (fig. 5).

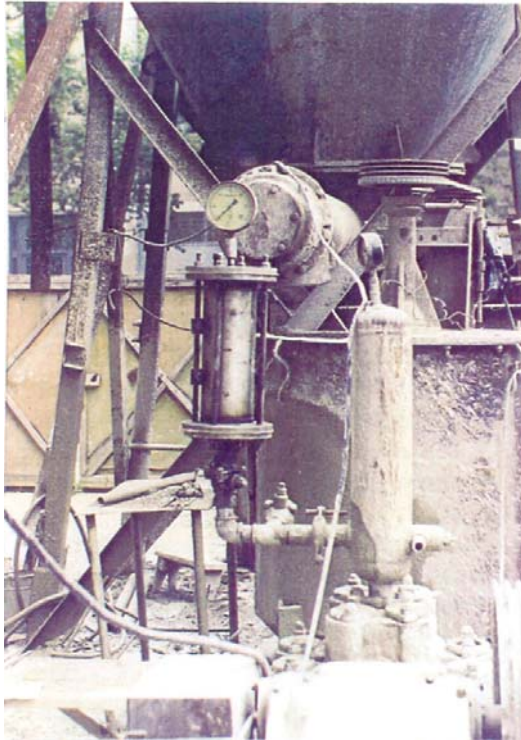


Fig. 3. The process of cement grout injection into a metallic cylindrical form



Fig. 4. Testing of freshly-placed concrete in a plastic form under the prolonged action of pressing

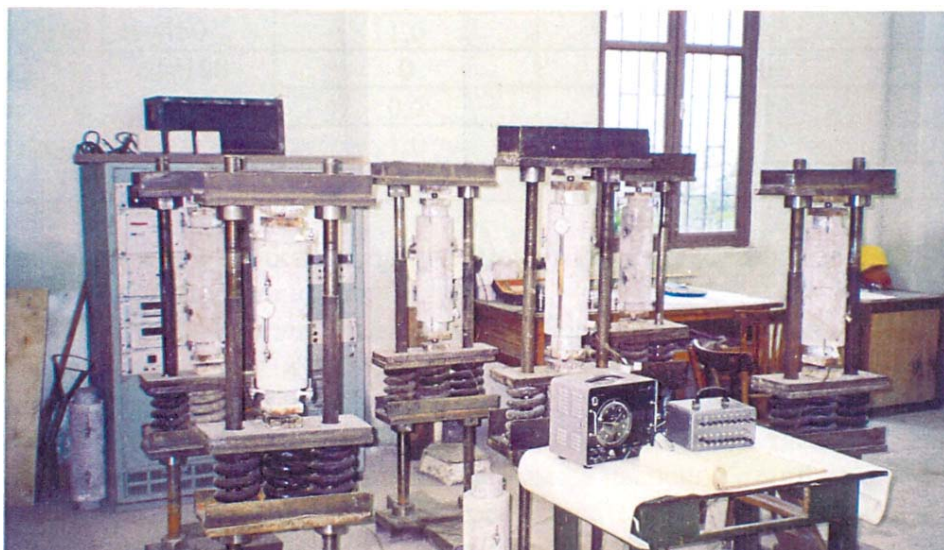


Fig. 5. Testing of freshly-placed concrete in a reinforced concrete under the prolonged action of pressing

Three pieces of concrete discs of diameter 420 mm and 100 mm in height were moulded with the purpose to study the distribution pattern of prestress occurring in vessel body roof and floor, induced by the stretching-out of a pair of curvilinear tendons embracing each semiperimeter of disk body and aligned in opposing directions. Bearing in mind the specific nature of disk testing, on the circular surface, 4x10 mm borders were being made provision for, in the process of disk moulding to ensure safe placement of reinforcing steel in testing. The stretching-out is taken as a

modelling of the stretching out that occurs due to the motion of the outer shell in result of cement grout injection in air-tight gap available in vessel body wall. Furthermore, the deformation noted along the length of the tendons makes it possible to ascertain the pattern of force variation both in the linear section and in curvature zone (fig. 6).

With a view to verifying the proposed technology of vessel body wall prestressing as well as to assessing its stressed state, two reinforced concrete cylindrical shells 1000 mm in height, 1050 mm and 920 mm in external diameter and 35 mm in thickness were concreted on a large compound cylindrical structural component (fig.7). In the cylinder with greater diameter, class A-III circular tendons the form of a spiral (8 mm of diameter and 25 mm pitch) were placed while in the cylinder with smaller diameter – tendons with 50 mm pitch. In a shell of greater diameter, at a distance of 100 m from the end, in its lower part, inlet connection union was made provision for, reaching its inside surface. On the outer side, there was a valve attached on the connection union for the fixation of the injected cement grout.

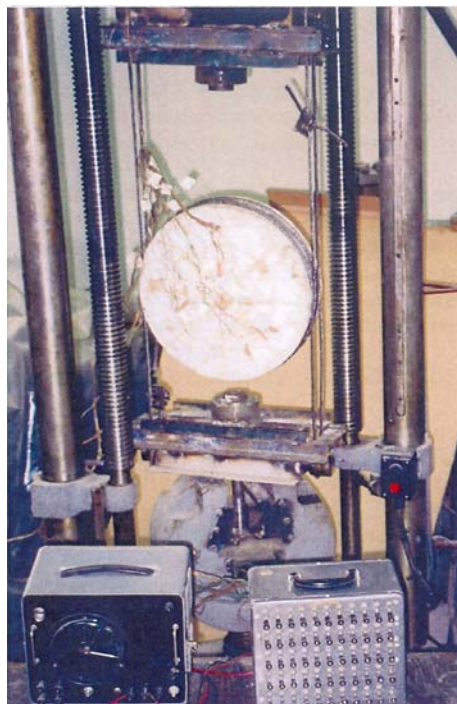


Fig. 6. Testing of reinforced concrete circular disk



Fig. 7. Reinforced concrete cylindric shells of compound frame wall

A month after cylindrical shells were made, operations were initiated involving the construction of a compound structural component of vessel wall. The shell with smaller diameter was placed inside one with a larger diameter, thus creating a gap of 30 mm in between.

Prior to creating air-tight gap, coupled welded rings of A-III class tendons (12 mm in diameter) have been installed in the upper and lower parts of the external surface of the outer shell in order to restrict its motion in radial direction in the course of compressive prestressing, as well as to upgrade gap leak-tightness reliability. The welded rings were made snug against the cylinder surface by filling up the designed 1 cm gap with expanding alunite cement grout.

After the placement of one shell into another, with a view to creating an leak-tight gap, originally in the lower part of the gap along the whole length of its circumference, a 100 mm plug made of alunite expanding cement has been arranged to reach the bottom of the inlet pipe - union. Two days later, a specially manufactured steel spiral 25 mm in diameter, with a 8 mm lead of a helix (wire diameter - 1 mm) was placed into the gap over the entire surface of the lower plug with a view to ensuring subsequent uniform filling - up of the gap with the grout injected. The gap was then filled up with crashed stone following which a similar upper plug was arranged with suitably-threaded tubes secured, enabling one to fasten two valves for air release at cement grout injection and gap filling-up monitoring as well as to mount a manometer for noting gap pressure.

In the process of specimen concreting, for the determination of strength and strain characteristics of the concrete, by the moment of testing, cubes 100x100x100 mm and prisms 100x100x400 mm were being moulded simultaneously.

### 3. Structural components testing

The properties of concrete (GAC), hardening in the gap between the outer and inner shells of vessel body, e.i. in a confined space, have been studied with test cylinders specimens at varied rigidity of casing section.

A metallic cylinder has been used as a casing, and so was a plastic tube. The casings were prefilled with crashed stone in fraction sizes 10...20 mm; thereafter, cement grout was being fed with a plasticizer (LST), its composition being 1/0.35/0.0025 (cement/water/plasticizer).

Cement grout injection into air-tight metallic forms has been performed at cementation station of the trust Gidropsstroy (Fig.3) developing pressures up to 2 Mpa.

The cement grout produced in mixer was fed into pumping station and then injected into steel form prefilled with crushed stone. Once the mix had flown out through the valve, which is an indication of air release and form filling-up with cement grout, the valve was shut off. Cement grout injection continued until the required pressure was attained, the monitoring being performed by a manometer at the pumping station and a manometer on the metallic form, whereupon the valve was shut-off. The form was then removed and another one was installed. The experiment envisaged three levels of head pressure - 0,5; 1,0 and 1,5 Mpa with two specimens prepared for each pressure level. Strength test of concrete cylinders at twenty-eight days will be performed by subjecting them to crashing on a hydraulic press. In Table 5 are represented the mean results of tests performed with two specimens for each pressure level.

Concrete specimen hardening in plastic casings proceeded under pressure in spring devices.

Spring device is a unit consisting of a system of rigid cross-pieces, tie-rods and springs (fig. 4).

Table 5

The results obtained for concrete hardening in casings under pressure

Casing type and its characteristics	Dimensions, mm	Pressure level, MPa	Concrete cylinder strength $R_{cyl}$ , MPa	$R_{cyl}/R_{cyl}^0$
<b>Metal</b> $\delta = 3.0$ mm; $E = 209500$ MPa	d=150 H=450	0	15.9	1.00
		0.5	18.8	1.18
		1.0	22.3	1.40
<b>Plastic</b> $\delta = 3.0$ mm; $E = 3700$ MPa	d=100 H=400	0	13.0	1.00
		0.5	20.1	1.55
		1.0	22.7	1.75
		1.5	19.3	1.48

The design force was applied to specimen punches by portable hydraulic jack connected to pump station as well as by springs and fixed with nuts available on tie-rods. The pressure applied was being monitored by a manometer mounted at the pump station.

To eliminate adhesion between the hardening concrete and phasing bottom and punch, polyethylene film was placed in between. After 30 days, the specimens placed in spring device were off-loaded and tested on hydraulic press. Average test results (for two specimens) are represented in table 5.

Reinforced concrete casings filled with crashed-stone and cement grout, with punches at either end, were placed in the above-mentioned spring devices with the purpose of the investigation of the prolonged deformations (creep and shrinkage) of concrete hardening under pressure as well as the determination of prestress losses induced by this process.

The values of pressure applied to freshly-placed concrete came up to: 1,64; 1,97; 2,62; 3,28 and 4,59 Mpa (fig. 5).

The movements of the punches in the process of specimens' loading as well as in time were determined by comparators with standard gauge length of 400 mm on steel studs with rolled-in steel balls at the ends, that had been secured to the punches on two diametrically opposite sides. Lengthwise deformations of a cylinder on 200 mm gauge length with concrete hardening under pressure were also measured by a comparator with standard gauge length of 150 mm, whereas the transverse deformations in the process of stress transfer to the concrete were measured by electronic resistance transducers with 50 mm gauge length, that had been glued in the mid-section of the test cylinder.

Temperature strains and shrinkage strains were being determined on two off-loaded twin specimens by means of a comparator with 150 mm base.

In compliance with the scheme suggested for the reinforcement of the floor and the roof of the vessel body, a set of experiments have been carried out to determine the pattern of stress distribution both in concrete and in the curvilinear section of tendons after they have been stretched out in the course of frame three-layer wall prestressing. The experiments were performed on a 100 mm thick concrete disks 420 mm in diameter, encircled by one pair of curvilinear tendons, through which the load was transferred to the disk concrete. In order to provide disk balance when transmitting load from tensile-testing machine to concrete by means of hinge-joint device, each branch of the pair under investigation was designed to consist of two tendons with curvilinear sections symmetric about the central plane of circular section (Fig.6).

By the beginning of testing, concrete strength and the modulus of elasticity, determined for control test cylinders, were found to come up to 12.1 MPa and 14500 MPa, respectively.

The first stage involved the investigation of the pattern of stress distribution along the disk circular contour, the load being transferred by tendons with frictional forces between concrete

and tendons available. With this object in view, class - A bars 8 mm in diameter have been employed with a curvilinear section within disk contact zone.

In order to reduce friction between tendons and concrete, a 1 mm steel zinc-plated sheet has been interlaid. The force exerted by tendons at various points of contact (with disk) in the course of testing has been evaluated by deformations measured by resistance strain gauges cemented to the surface of the reinforcing bars both within the contact zone and outside it.

The load applied to the reinforcing bars has been increased by steps.

When the relative deformation measured beyond the boundaries of disk zone amounted to an average of  $50 \times 10^{-5}$ , which corresponded to the load of 20 kN and tendon stress of 105 MPa, the experiment was terminated because of the risk of tendon rupture in the section deteriorated by the thread at the point of its fixing to the spherical hinge-device.

In the second stage of the experiment the pattern of stress distribution in the body of concrete disk has been determined, the said stresses being brought about by the compressive force arising in the curvilinear section of the pair of tendons under tension. At this stage, the plain bars have been replaced by circular cable 8 mm in diameter, passed over the spherical hinge device to ensure the application of symmetrical load to the concrete disk.

The magnitudes of compressive stresses have been obtained from the readings of resistance strain gauges cemented to the flat surface of the disk for all stages of disk loading both in tangential and radial directions.

The technology of high-pressure body compressive stressing has been studied on a thick compound large-scale cylindrical component, the latter being a spacial construction consisting of two coaxially-positioned cylindrical reinforced concrete shells with a 30 mm gap in between, filled up with GAC concrete.

The experiment involved two stages.

The first stage involved the study of the stressed-strained state of a three-layer wall of a structural unit at cement grout injection into the gap filled up with crushed stone as well as in the course of concrete hardening in confined space under pressure (Fig.8).

By the beginning of structural unit testing, the shell concrete strength determined with control test cylinders was 20.5, and the modulus of elasticity was 16500 MPa.



Fig. 8. Injection of cement grout into the gap of compound frame wall

On the third day, after arranging the upper plug, the gap was prefilled with water for wetting the crushed stone lying inside, as well as for checking the control valves and manometer for safe operation. Thereupon, once the water has been discharged, cement grout of mix proportions:

1/0.35/0.0025 was being injected at a pressure of about up to the point when it started flowing out from the open valves, following which the latter were being closed. The pressure was then brought up to 0.3 MPa and maintained constant by pumping up the mixture with grouting pump until manometer indications have been stabilized.

Once the spherical valve fitted on the inlet pipe-union has been closed, the pressure level attained remained unchanged.

The deformations of the outer and inner shells of the prestressed structural unit were recorded by comparators at points specified in testing program as well as by Huggenberger tensometers placed on a 100 mm base in the central section of structural unit shells equally offset from the areas monitored by the comparators (on 180 mm base).

The first crack has been detected on the outer surface of the structural unit at a gap pressure of about 0.15 MPa. As the pressure increased, the number of cracks increased as well. On the inner surface of the structural unit compressive strains have been detected.

The second stage of the experiment involved the testing of the prestressed structural unit for internal hydrostatic pressure to evaluate the effect anticipated.

This was done by proceeding as follows: 20 mm thick metallic cylinder shell has been placed inside the structural unit with a 30 mm gap for producing internal pressure on the structural unit under test. By analogy with the described above, plugs were fitted at the upper and lower parts of the gap. In the cylinder shell two union-pipes were arranged level with the bottom of the upper plug - one for water supply to the air-tight gap created, and the other one - for mounting a valve intended for air release from the gap over the period of time required for prefilling.

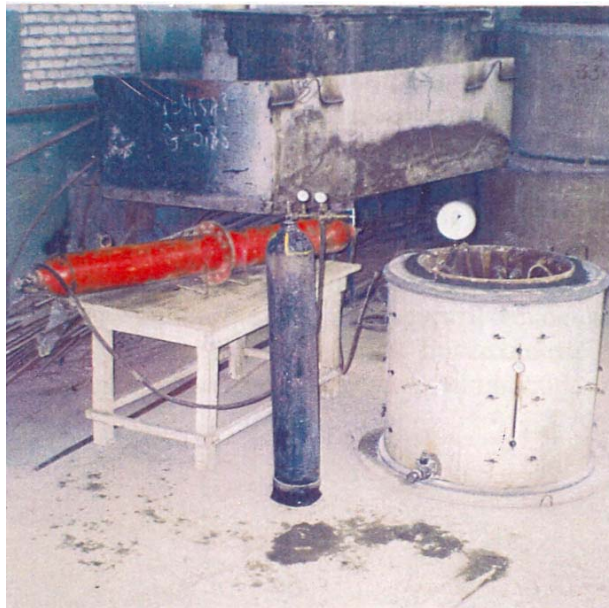


Fig. 9. Testing of compound prestressed frame wall for inner hydrostatic pressure

The internal hydrostatic pressure was produced by compressed air available in a cylinder. The compressed air was supplied through a high pressure hose to a feeding device prefilled with water. The water was then injected under pressure into the gap between the cylinder shell and the structural unit tested. The magnitude of the pressure was being monitored by a manometer mounted on the feeding hose by means of a tee-joint (Fig.9). There was a stepwise increase (by 0.1 MPa) in the pressure exerted on the structural unit tested. At each step, the pressure was

maintained constant for about 10-15 minutes required to examine the state of structural unit outer surface as well as to note the readings of the devices installed and to measure the width of crack opening. The hydrostatic pressure was being raised until wet stain appeared on the outer surface of the structural unit, its magnitude constituting 1.0 MPa. This load is indicative of the commencement of cracking over the inner surface of the structural unit.

#### 4. Model testing

The results of the experiments cited above have lent support to the advisability of employing the technology for compressive stressing of three-layer shell. The prime object of the experiment with vessel model was to reveal the effect of the compressive stressing of cylindrical closed shell inner layer by creating pressure in the gap rather than to ascertain compressive stressing technique. Since the specified model gap (10 mm) did not allow for the creation of compressive stressing using the technology developed, pressure was applied by means of expanding cement alunite grout. This kind of technique was being used in carrying out repair work on Enguri waterpower plant diversion tunnel (Georgia), 9,5 m in diameter. The said method is widely used in the United States (expanding cements K, M and S).

Before the placement of cement grout into the model, an implementation of some supplementary tests has been found necessary for the determination of expansion coefficient, the influence of rigidity ("bound spacings") etc. on the magnitude of compressive stressing.

An investigation was conducted with cement grout of composition 1:0,3 (cement:water) and plasticizer LST - 0,3% of cement mass. The intent in using the plasticizer was to reduce toughness and slow down cement setting.

The expansion of "free specimens" was being studied with prism 40x40x160 mm (fig.10). Experimental results have shown the expansion to be occurring on the first day and coming up to 4,2%, which constitutes 92% of total expansion during 72 hours (4,55%).

The expansion of "bound specimens" was studied on ring-shaped specimens of height 160 mm with inner ring external diameter of 442 and outer ring internal diameter of 462 (fig.11). The gap between these rings was filled with blended alunite cement grout. The equal amounts of the expanding cement in the gap, i.e. equal energy of expansion released in cement hardening, make it possible to access the value of pressure on casing rings in accordance with the rigidity of their section.

Differing magnitude of rigidity for "bound specimens" (rings) was provided by the application of different materials - on one occasion, 2,7 mm thick acrylic plastic with elasticity modulus of  $E=3500$  Mpa and ultimate strength  $R=61,0$  Mpa and on another occasion - aluminium alloy sheet 1 mm in thickness, with the modulus of elasticity  $E=56000$  Mpa and ultimate strength  $R=367$  Mpa. The choice of aluminium for a casing was dictated by the near match between the rigidity of the experimental specimen and that of vessel model.

Simultaneously, the influence of the temperature released in the course of expanding cement hardening on acrylic plastic was being investigated on free specimens 200x200x10 mm. On the surface of specimens a sheet of acrylic plastic was placed, with Huggenberger tensometer mounted.

The values of relative deformations within 7 days were no greater than  $3 \cdot 10^{-5}$ , i.e. the influence of temperature on the deformation of ring type casings was not actually detected.

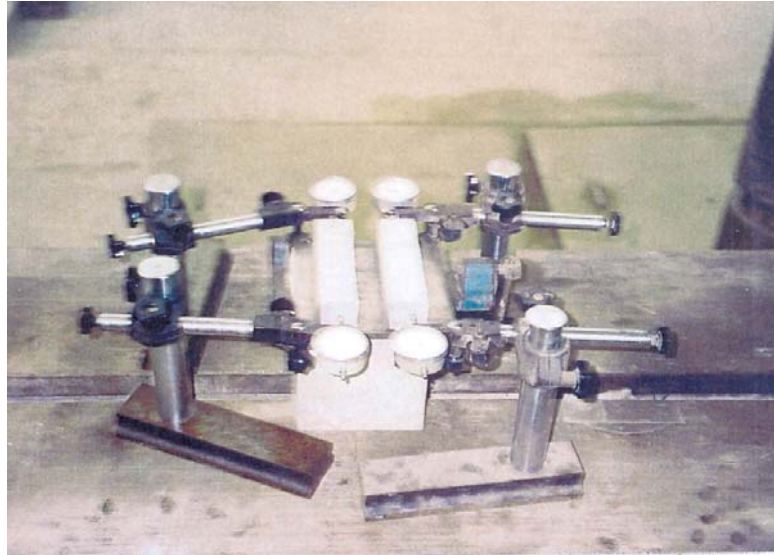


Fig. 10. The study of "free specimens" expansion

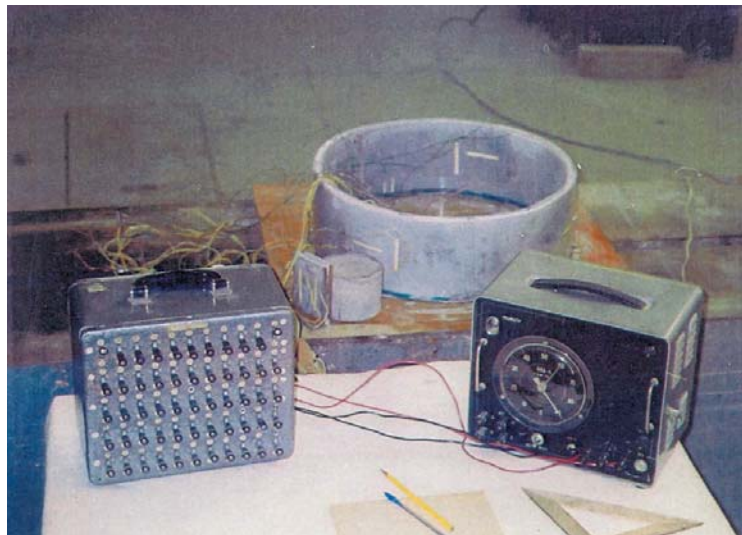


Fig. 11. The study of "bound specimens" expansion

In the course of "bound specimens" testing, electric resistance transducers with base of 50 mm, pasted evenly along the circumference in the central part of the specimen, were employed to measure both tangential and vertical deformation of the inner and outer rings.

After the above-mentioned experiments have been completed, the frame model itself was tested. The experiment involved two stages.

The first stage involved the prestressing of the inner section of the frame by injecting the expanding blended alunitic grout into the gap between cylindrical shells (fig.12). The magnitude of free expansion has been determined from prism 40x40x160 mm tests carried out concurrently with the principal test.

The stressed and strained state of the model in the process of compressive stressing was examined by means of electronic resistance transducers with 20 mm base, pasted in advance (with regard for preparation technology) to the inner surface of the floor, roof and outer shell.

At the second stage, with deformations becoming stable (on the seventh day), the prestressed model was put to compressed air - produced hydrostatic pressure tests (fig.13). Compressed air was supplied from the cylinder through high pressure hoses to the feeding device prefilled with water entering the internal section of the model. After model filling up with water, test pressure gauge was fitted on its roof for pressure monitoring.



Fig. 12. Prestressing of the frame model

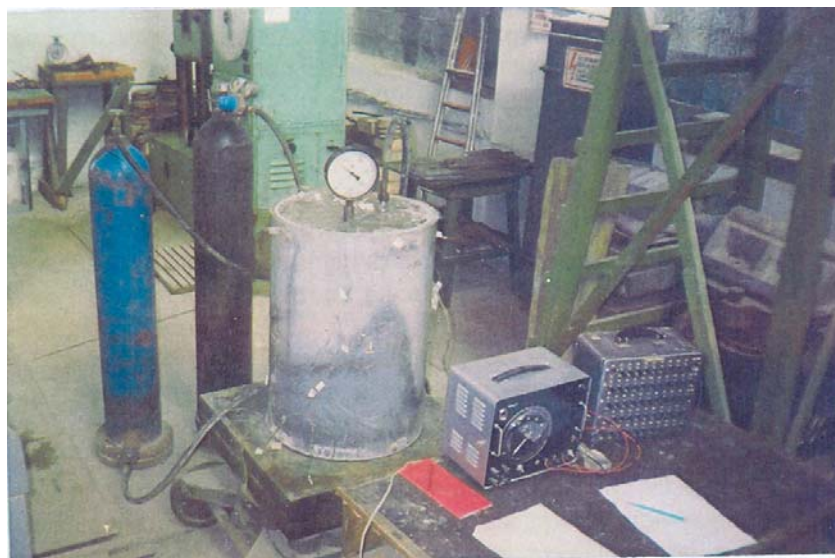


Fig. 13. Testing of prestressed frame model for inner hydrostatic pressure

The pressure was raised in steps with 10-15 min delay at each step - the time it took to note deformation readings (with АИД-2 device) (fig.13). On achieving the internal pressure of 0,4 Mpa, the model was unloaded in a step-wise manner down to conventional zero (0,05 Mpa). The pressure having been raised after some delay in a step-wise manner up to 0,5 Mpa, the test was completed and the pressure released.

## 5. An analysis of experimental data

A detailed analysis of the experimental data obtained made it possible to establish the pattern of the influence of some factors on the compressive prestressing of the proposed high-pressure vessel structural unit as well as to evaluate its stressed and strained state through the use of the design technique devised.

The investigation of the behaviour of concrete (GAC) placed in a closed space and hardening under pressure revealed the impact of the form-casing rigidity on its maximum strength. Relying on the data provided by some other researches, a relationship between concrete strength growth and the pressure has been represented in a graphical form in fig.14 [11]. It can be seen from the diagram that as the pressure increases, concrete strength at first increases up to a certain magnitude and then decreases, this pattern being determined by the casing rigidity.

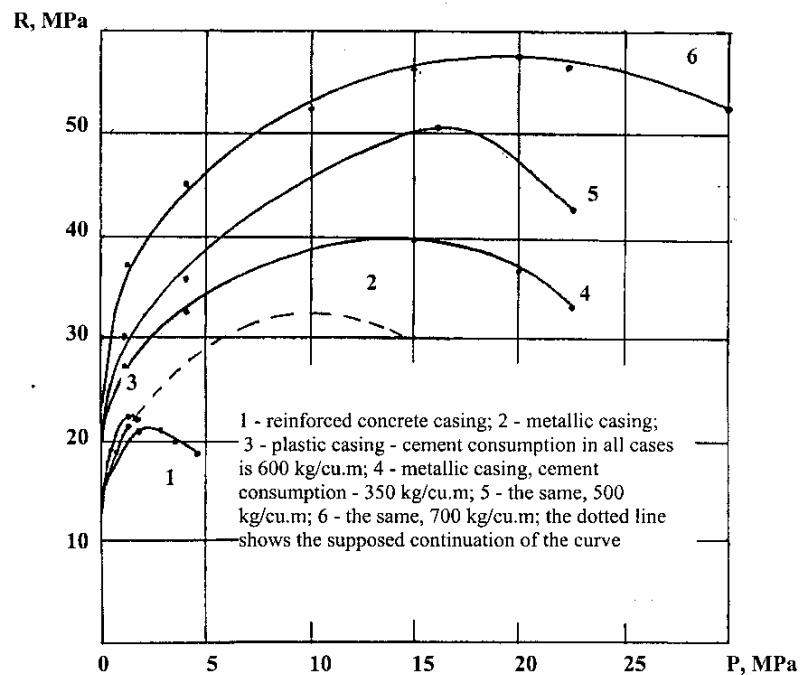


Fig. 14. Concrete strength-pressure relationship

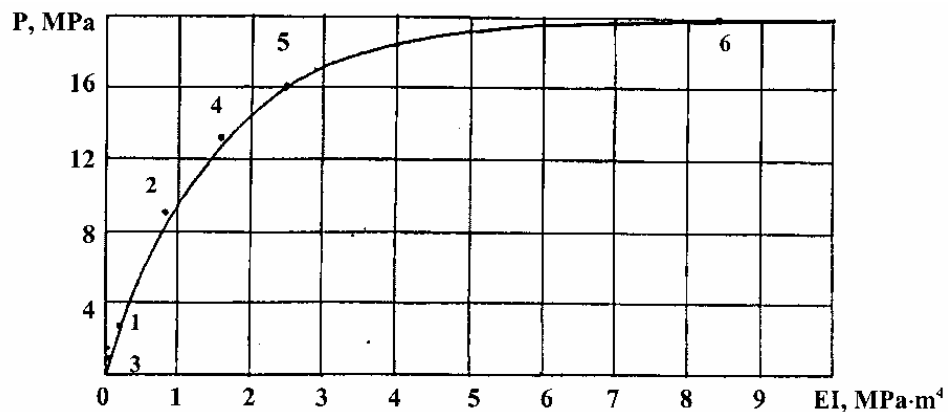


Fig. 15. Effective pressure on freshly-placed concrete - form rigidity relationship  
 Point numbers correspond to the curves in fig.14

The relationship between strength and the effective pressure exerted on the freshly-placed concrete that is essential to attain maximum strength, depicted in fig.15, takes the following form:

$$P = 20(1 - e^{-0,65EI}),$$

with P - pressure, MPa; E - modulus of elasticity for casing material, MPa; I - the moment of inertia of casing cross-section, m<sup>4</sup>.

The prestress magnitude of the structural unit of a high-pressure vessel is directly associated with the processes occurring in time in concrete placed in the gap between cylindrical shells under pressure, namely, with creep and shrinkage, that were being investigated on specimens placed in reinforced concrete casing, at five levels of compressive prestressing of freshly-placed GAC concrete.

Creep deformations were determined by subtracting temperature and shrinkage strains noted on off-loaded specimens from the total deformations. The results thus obtained are represented in fig.16.

Prestress losses concrete were determined by noting pumping station manometer readings at specimen off-loading (after 85-90 days, with deformations stabilized) at the moment of spring device fixing nuts' loosening as well as by measuring deformations at concrete off-loading. The magnitude of the losses was judged by the difference in stresses at loading and off-loading.

In table 6 are given the results of investigations aimed at the determination of prestress losses.

Table 6

№ of specimen	Compressive stressing, $\sigma_{com.stres.}$ , MPa	Elastic off-loading, $\varepsilon_{y.p.} \cdot 10^5$	Shifting of nuts, $\sigma_B$ , MPa	$E_B$ , MPa	$\varepsilon_{y.p.} \cdot E_B$ , MPa	$\sigma_{com.stres.} - \sigma_B$ , MPa	$\sigma_{com.stres.} - \varepsilon_{y.p.} \times E_B$ , MPa	Losses	
								Mean, MPa	%
1	4,586	23,0	3,934	17200	3,956	0,654	0,630	0,642	14,0
2	3,277	17,7	3,082	18000	3,186	0,195	0,097	0,146	4,8
3	2,621	10,3	2,229	24000	2,459	0,392	0,162	0,277	10,0
4	2,621	10,5	2,496	24000	2,486	0,196	0,125	0,360	13,5
5	1,966	9,1	1,638	20600	1,872	0,328	0,094	0,211	10,7
6	1,638	7,0	1,311	22500	1,575	0,327	0,065	0,196	12,0

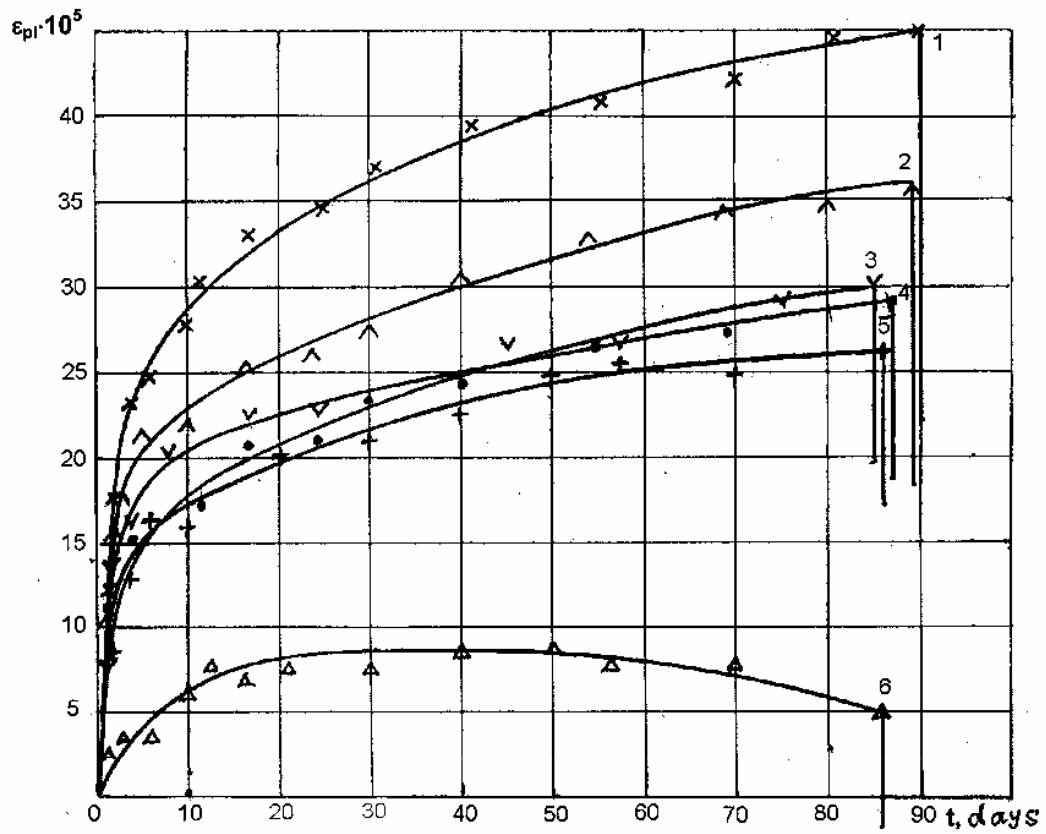
As may be seen from the table, prestress losses do not exceed 15% of initial stress, so this value can be recommended to be used in designing.

The experimental investigation of the stressed-strained state of concrete disks representing the resistance of vessel body roof and floor at the moment of their compressive stressing with tendons as well as the pattern of force distribution over the curvilinear tendon section in the process of its stretching-out has shown the intensity of tendon pressure along disk circular contour to be varying smoothly from its maximum value of  $N_0$  at the beginning of contact down to  $0,57 N_0$  in its medium point (fig.17).

The change in tendon forces may be determined from the following formula

$$N_0 = N_0 - e^{-\beta\theta}$$

a)



b)

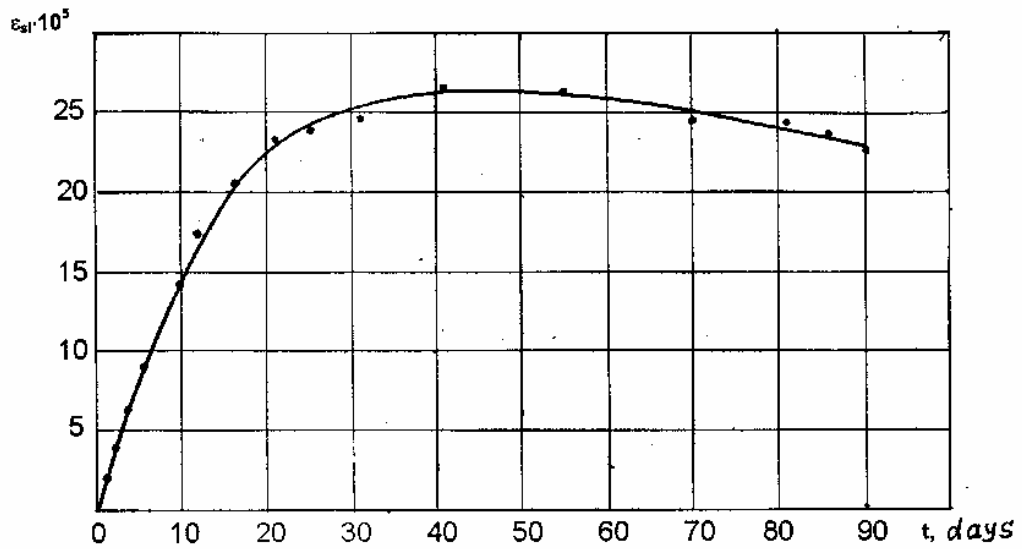


Fig. 16. Concrete deformation variation in time:  
 a) creep; b) shrinkage and ambient temperature: Pressure on test specimen, MPa: 4,59 (1); 3,28 (2); 2,62 (3); 2,62 (4); 1,97 (5); 1,64 (6)



with  $N_0$  – tendon force over the linear section with no contact with concrete:  $\mu$  – tendon friction coefficient (on the surface, in our case on galvanized sheet  $\mu=0,35$ );  $\theta$  - polar coordinate;  $\theta < \theta \leq \pi/2$ .

Fig.18 includes radial and tangential stresses in disk body. As can be seen from the figure, disk surface is characterized by ununiform distribution, which can be attributed to the fact that in the zone of the contact with tendon, all through the disk thickness, local stresses are created, their redistribution throughout the thickness occurring gradually towards the center, the phenomenon being represented in diagrams by convexity. The experiment on vessel wall structural unit prestressing following the technology proposed has confirmed the effectiveness of this method. It has been found that the grout mix used, the one that had been tested on cylindrical specimens, may be used for this purpose.

The readings of comparators and tensometers mounted on the external and internal surfaces of structural unit compound wall were used in the determination of their deformations under cement grout injection and also in the process of concrete hardening. Fig. 19 and 20 represent the mean relative tangential deformations for various levels of the shells.

As can be seen from fig.19, at a pressure of 0,3 MPa on the inner surface of the structural unit, tangential compressive strains in mid-zone are somewhat greater than in the upper and lower zones, which can be accounted for by an edge effect. The lower zone appeared to be more restricted due to friction on the laboratory floor the structural unit had been installed on. With a pressure in the gap reaching 0,15 MPa, the first crack has been found to be occurring on the external surface of the structural unit. By that time the mean tensile strain has reached the value of  $13 \cdot 10^{-5}$ . The number of cracks increased with increased pressure. After the injection has been completed the mean tangential compressive and tensile deformations of the structural unit came up to  $23 \cdot 10^{-5}$  and  $29 \cdot 10^{-5}$ , respectively.

Within 31 days of structural unit prestressing, it has been tested for internal hydrostatic pressure. Before testing, structural unit inner shell compressive stress deformation was  $20 \cdot 10^{-5}$ , e.i. prestress losses amounted to about 14 percent.

As the pressure increased in a stepwise manner (by 0,1 MPa), the examination of the structural unit external surface revealed a wet patch occurring at the pressure of 1,0 MPa, which was an indication of the inception of cracking on the internal surface. The experiment was then discontinued by releasing the pressure.

The prestressing of vessel structural component following this procedure made it possible to ensure a four-fold increase in wall section crack-resistance with the structural component made of common concrete of the same brand (at  $R_{bt}=1,15$  MPa).

In preliminary tests, preceding the basic model study, the effect of compressive prestressing was being investigated, the said effect occurring in the process of expanding cement grout hardening in the gap between two rings of different rigidity.

Supplementary test results have shown the pressures on the external and internal rings to be different as opposed to the pressure produced by injecting common portlandcement into a closed gap, with both surfaces experiencing equal pressures. The external ring was exposed to a higher pressure. Both rings simultaneously experience tensile stresses acting lengthwise, that is along their generatrices, due to a close contact with the expanding cement, the outer ring being less stressed than the inner ring.

While discussing with the collaborator the effect observed to make sure, once again, that the test results are valid, a decision was made to carry out a second experiment. With this purpose in view, identical specimen rings were fabricated and tested, all relevant preliminary investigations of parameters (overall dimensions, grout composition, material) being duly accomplished.

Experimental data processing has shown the results of the two series of tests to be virtually in complete agreement (fig.21 and 22). The pressure distribution pattern obtained can be, to all

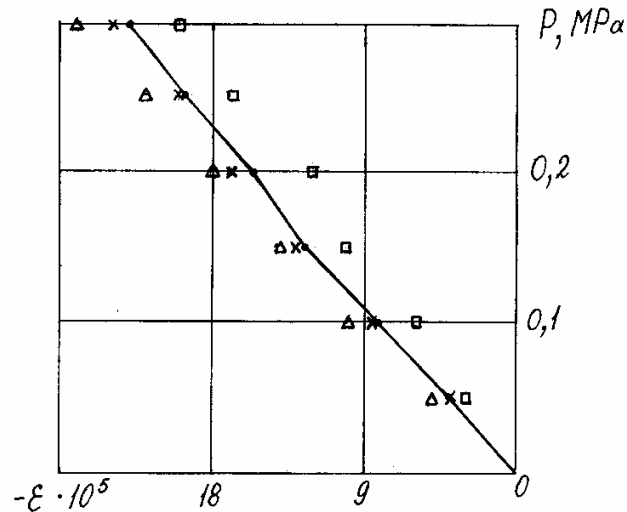


Fig. 19. Discharge pressure dependence of the tangential deformations of structural unit's compressed inner shell:

$\square$  - lower zone;  $\Delta$  - mid-zone;  $\times$  - upper zone;  $\bullet$  - mean deformations

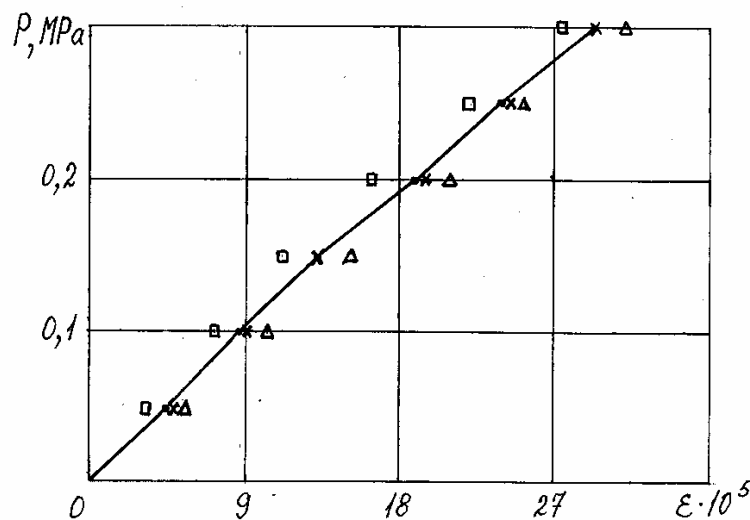


Fig. 20. Discharge pressure dependence of the tangential deformations of structural unit's stretched outer shell (Designations are the same as in fig. 19)

appearances, explained by the peculiarity of expanding cement hardening under the restricted conditions of the ring casings.

The progress of deformation development in the external and internal rings was being observed for seven days. The deformations (cement expansion) have been found to be increasing mostly during the first 24 hours, following which only a slight increase in deformations (3-5%) was observed, signifying the occurrence of stabilization. This is why fig. 21 shows the development of deformations in the form of mean values obtained during the first 24 hours from two different experiments. As can be seen from the graphical diagram, in 15 hours' time, about 90% of all the deformations recorded have been found to be stabilized. 24 hours later the relative tensile deformation in a ring with acrylic plastic and aluminium casings came up to  $85 \cdot 10^{-5}$  and

$42 \cdot 10^{-5}$  respectively, while relative compression deformation –  $63 \cdot 10^{-5}$  and  $32 \cdot 10^{-5}$ , i.e. tensile deformation appeared to be greater than compression deformation by 35% in a ring with acrylic plastic casings and by 31% - in a ring with aluminium casings. Under hydrostatic pressure this difference is 6% and 5%, respectively.

Based on the values of relative tangential deformations, the values of pressures inducing these deformations have been determined. It has been found, that as compared to hydrostatic pressure, the pressure acting on the outer ring casing exceeds the pressure acting on the inner ring casing: for acrylic plastic – 27, for aluminium – 25%. The diagram in fig. 22 represents the dependence of these pressures on the specific rebuff factor for the corresponding casing ring  $K_0 = E\delta/100r$  (N/cu.cm), with E, r and  $\delta$  – modulus of elasticity (N/cu.cm), radins and casing thickness, cm.

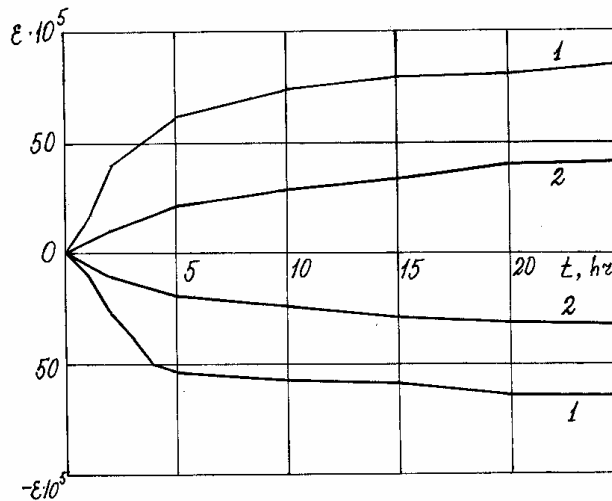


Fig. 21. Time variation of casing ring tangential deformations in the course of expanding cement hardening: 1 - acrylic plastic; 2 - alluminium

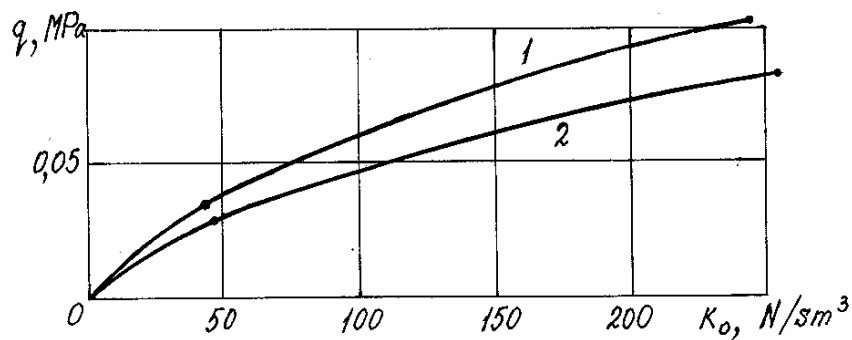


Fig. 22. Expanding cement-produced pressure - specific ring resistance relationship:  
 1 - outer ring; 2 - inner ring  
 • - acrylic plastic; × - alluminium

The results obtained confirmed the possibility of expanding cement application for creating compressive prestress of model inner shell, which was duly done.

As may be seen from a diagram in fig.22, with increased  $K_0$ , the pressure on casing walls may increase up to a certain limit after which the effect just dissapears, which means that an increase in cement expansion deformations should not exceed a certain value at which sufficient prestress forces may occur.

Since in the process of cement grout hardening, its volume increases considerably at an early stage, constraining its deformations in one or two directions, it will try to expand in an unrestricted direction.

In our experiments, in constraining cement deformations in both radial and tangential directions, part of expansion energy was released towards the free ends of the gap. In so doing, due to the contact of cement with the casings as well as to the pressure acting on them, the latter underwent tensile deformation along the casing rings' generatrices owing to cement expansion. In the inner and outer casing rings, subjected to different pressures, there were different deformations noted along their generatrices. In the outer rings which were subjected to greater pressure, these deformations were manifested in a lesser extent than in the inner rings. By the end of 24-hours, the mean values of deformations in the outer casings of acrylic plastic and alluminium were  $57 \cdot 10^{-5}$  and  $26 \cdot 10^{-5}$ , respectively, and in the inner casings –  $77 \cdot 10^{-5}$  and  $36 \cdot 10^{-5}$  (fig.23), i.e., in the inner casing they were greater by 35% than in the outer casing.

The strains occurring in the cylindrical shells after the stabilization of cement expansion in the gap between them can be judged by tangential deformation measurements in the circular mid-cross-section of the model. However, the comprehensive theoretical investigation involved the determination of the magnitude of pressure in the gap inducing tensile stresses in the outer cylinder and compressive stresses in the inner cylinder.

Taking into consideration the fact that the same grout of expanding cement has been used for the vessel model, that is, the grout featuring the same properties was placed in a similar gap (10 mm) with practically identical gap radii, the magnitude of pressure was determined (amounting to 0,095 MPa and 0,078 MPa) relying on the values of  $K_0$  calculated for outer and inner cylindrical shells, 209 N/cu.cm and 233 N/cu.cm, respectively.

In order to assess the stresses occurring in model wall along cylindrical geriatrices associated with the property of cement expansion under confined conditions, longitudinal relative tensile strains noted in the model on the outer and inner cylindrical shells ( $27 \cdot 10^{-5}$  and  $38 \cdot 10^{-5}$ , respectively) have been taken into consideration, that is the stresses of 1,0 MPa and 1,4 MPa (fig. 13 and 14).

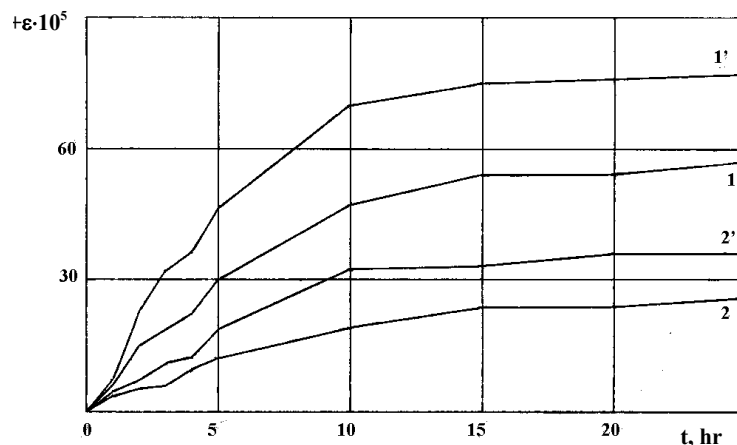


Fig. 23. Changes in casing ring relative deformations with time along their generation in the process of expanding cement hardening:

1, 1' - Acrylic plastic outer and inner casings; 2, 2' - Alluminium outer and inner casings

The analysis made also allowance for the action of internal pressure (P) on the prestressed vessel model. Theoretical investigations were carried out based on a three-dimensional model following finite-element method with due regard for the condition of symmetry.

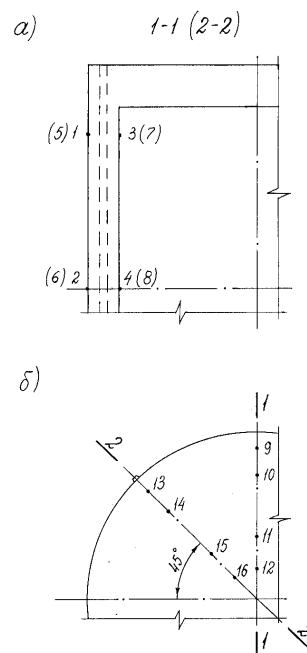


Fig. 24. The layout for the position of the points wherein the stresses have been noted

In tables 7 and 8 are represented the results of vessel body model tests in the form of stresses along two vertical sections running through tendon anchor and outside it, with prestress as well as with internal pressure available. The same tables include the stress values for corresponding points of the section so that appropriate correlation can be done.

Table 7 gives tangential stresses (MPa) in model cylindrical shells and table 8 offers stresses in the radial and tangential directions of the plate (roof). From tables 7 and 8 it can be seen that there is a sufficiently good agreement between the experimental values and the calculated ones and isolated deviations (for example in points 5 and 14) should be attributed to the errors made in experiments.

Table 7

Vertical section	№ of points	Under prestressing		At internal pressure, MPa				Total			
		exper.	theor.	0,2		0,4		0,2		0,4	
				exper.	theor.	exper.	theor.	exper.	theor.	exper.	theor.
1-1	1	1,90	1,88	-0,15	-0,13	-0,36	-0,26	1,75	1,75	1,54	1,62
	2	1,75	1,74	0,88	0,81	1,86	1,62	2,63	2,55	3,61	3,36
	3	-0,87	-1,02	-	0,38	-	0,77	-	-0,64	-	-0,25
	4	-1,57	-1,37	-	1,31	-	2,62	-	-0,06	-	1,25
2-2	5	1,46	1,49	-0,18	-0,13	-0,44	-0,26	1,28	1,36	1,02	1,23
	6	1,86	1,71	0,88	0,81	1,79	1,62	2,74	2,52	3,65	3,33
	7	-0,80	-1,02	-	0,38	-	0,77	-	-0,64	-	-0,25
	8	-1,64	-1,37	-	1,31	-	2,62	-	-0,06	-	1,25

Footnote: The position of the points is shown in fig.24,a

The stresses given in table 7 are indicative of model cylinder internal shell compressive prestressing at the expense of the pressure produced in a gap of its wall which practically disappears under internal pressure of 0,2 Mpa.

The examination of the results (table 8) obtained shows that the prestressed tendons of the plate (roof and floor) in experimental model, placed in its mid-layer, produced a favourable effect.

For this effect to be intensified and performance of vessel structural unit to be improved, these tendons should be placed at the external surface of the plate relieving the tensile stresses.

As for the use of the expanding cement for prestressing of this kind of structural unit, account should be taken of the longitudinal tensile stresses occurring in cylindrical shells, that may exceed tangential stresses and consequently call for additional stress-checking arrangements.

Theoretical investigation of the model and subsequent correlation with experimental data have confirmed the efficiency of the proposed structural unit of high-pressure vessel.

Table 8

Ver- tical sec- tion	№ of po- ints	Under prestressing								At internal pressure 0,4 MPa			
		Internal surface				External surface				Radial		Tangential	
		Radial		Tangential		Radial		Tangential					
		exper	theor.	exper	theor.	exper	theor.	exper	theor.	exper	theor.	exper.	theor.
1-1	9	-0,36	-0,45	-0,51	-0,45	0,07	0,02	0	0,02	-0,73	-1,31	1,10	0,77
	10	-0,29	-0,31	-0,25	-0,34	0,11	0,08	0,04	0,08	1,46	0,73	2,55	2,00
	11	-0,33	-0,30	-0,29	-0,30	0,04	0,06	0,07	0,06	4,38	3,74	4,38	3,98
	12	-0,33	-0,30	-0,29	-0,30	0,07	0,06	0,07	0,06	4,38	4,50	4,74	4,42
2-2	13	-0,40	-0,48	-0,47	-0,46	0,11	0,04	0,04	0,0	-1,10	-1,31	0,73	0,77
	14	-0,36	-0,30	-0,25	-0,34	0,14	0,08	0,07	0,09	1,46	0,73	2,92	2,00
	15	-0,36	-0,30	-0,29	-0,30	0,07	0,06	0,07	0,06	4,02	3,74	4,38	3,98
	16	-0,36	-0,30	-0,33	-0,30	0,04	0,06	0,07	0,06	5,11	4,50	4,74	4,42

Footnote: The position of points is shown in fig.24,b

## R E F E R E N C E

1. Polyakov L.P., Fineburd F.M. The modelling of structures. "Budivelnik", Kiev. 1975.
2. Preece B.W., Davies J.D. Models for structural concrete. CR Books Limited. The Adelphi, John Adam Street, London WC2, 1964.
3. All-Union State Standard 8736-93. Sand for construction operations. International scientific and technical commission on standardization and technical norms adoption in construction business. Minsk. 1995.
4. All-Union State Standard 8267-93. Crushed stone and gravel from dense rocks for construction work. International scientific and technical commission on standardization and technical norm adoption in construction business. Minsk, 1996.
5. BS 882:1992. Specification for aggregates from natural sources for concrete.
6. ASTM C-33-97. Specification for Concrete Aggregates.
7. All-Union State Standard 310.1-76. Cements. Test methods. General statements.  
All-Union State Standard 310.2-76. Cements. The methods for the determination of fineness.

- All-Union State Standard 310.3-76. Cements. The methods for the definition of normal density, setting dates and uniformity in the change of the volume
- All-Union State Standard 310.4-81. Cements. The methods for the determination of the ultimate strength under bending and compression
8. Brown K.A. A study of high-strength grout properties. FIP-RJLEM, Symposium, Trondheim, Norway, 1961.
  9. M.Polivka. Crouts for post-tensioned prestressed concrete members. FIP-RILEM, Symposium, Trondheim, Norway, 1961.
  10. Volter O. The variability of the grout at the building site. FIP-RILEM, Symposium, Trondheim, Norway, 1961.
  11. Elbakidze M.G., Erukashvili I.R. Pressing and vibropressing of cement grout, mortars and concrete. Izvestia TNISGEI, Moscow, Energy, 1971.
  12. The instructions for the implementation of concrete-handling operations. Moscow. Stroiizdat. 1975.
  13. All-Union State Standard 10180-90. Concretes. The methods for the determination of strength on control specimens. State construction committee, the USSR. Moscow.

**ARCHIL KUBANEISHVILI. Doctor of Technical Sciences, Professor, Georgian Research Institute of Power Engineering and Power Structures, 0171, Georgia, str. Kostava, 70.  
Tel.: +995(32) 38-67-98; Mob.: +995 99 939496  
E-mail: SPTC.Centre@gmail.com**